Int. J. Electrochem. Sci., 8 **(2013)** 5902 - 5924

International Journal of
ELECTROCHEMICAL
SCIENCE
www.electrochemsci.org

Electrochemical Corrosion and Mathematical Model of Cold Spray Cu-Cu_2O Coating in NaCl Solution — Part I: Tafel Polarization Region Model

Ding Rui[1,2,*], *Li Xiangbo*[1], *Wang Jia*[2,3], *Xu Likun*[1]

[1] Science and Technology on Marine Corrosion and Protection Laboratory, Luoyang Ship Material Research Institute(LSRMI), Qingdao 266101, China;
[2] Ocean University of China, Qingdao 266003, China;
[3] State Key Laboratory for Corrosion and Protection, Shenyang 110016,China
[*]E-mail: dmoyuyang@foxmail.com

Received: 19 January 2013 / *Accepted:* 28 February 2013 / *Published:* 1 April 2013

Cu-Cu_2O coating was prepared by advanced Cold Spray technology and rotating ring-disk electrode was applied to study corrosion behavior of the coating in 3.5% NaCl solution.The influence of electrode rotation rate, chloride ion concentration, temperature and pH on polarization of the coating was investigated. The results indicate that the corrosion behavior of Cold Spray Cu-Cu_2O coating in Tafel region was under control of both diffusion process and electrochemical reaction, and the limiting diffusion species was $CuCl_2^-$. The increase of [Cl^-] or decrease of pH accelerates dissolution of Cu_2O. This facilitates the release of toxins and improvement of antifouling effect. The rise of temperature accelerates diffusion processes, which weaken the role of diffusion domination and enhance the effect of electrochemical reaction. When the coating is immersed in seawater, three processes proceed in coating surface: (1) active anodic dissolution, (2) formation of the oxide film, (3) dissolution of the oxide film, which are parallel and competitive reciprocally. Based on the reaction mechanism, a mathematical model for anodic Tafel polarization of Cu-Cu_2O coating was established and corresponded with experimental results well.

Keywords: Cold Spray; Copper; Cuprous oxide; Electrochemical corrosion; Mathematical model

1. INTRODUCTION

In previous studies, the ship fouling situation and progress of long-lasting anti-fouling technology were analyzed. Cold spray Cu-Cu_2O anti-fouling coating was developed in order to solve

ship fouling problems[1]. Then the physical characteristics such as deposition effect and micro-hardness were discussed.

Antifouling function of Cold Spray Cu-Cu_2O coating is achieved through the release of Cu(I) and Cu(II) to the surrounding water, therefore, the study of the electrochemical corrosion properties of the coating is necessary[2,3]. Since the electrochemical corrosion of cold spraying Cu-Cu_2O coating relates to the corrosion of copper, many research have been done to studied it[4-7], and three different reaction mechanisms and corresponding mathematical models were developed[8-18], their mechanism were listed below (Table 1). However, the charge transfer process was usually assumed to be quasi-reversible in derivation process of these reaction mechanisms and mathematical models. This would put the diffusion process as the control step and could not reflect the real situation.

Mechanism 1[19-23]:

$$Cu + 2Cl^- \Leftrightarrow CuCl_2^- + e^-$$

Mechanism 2[11,12,15,16,24]:

$$Cu \Leftrightarrow Cu^+ + e^-$$

$$Cu^+ + 2Cl^- \Leftrightarrow CuCl_2^-$$

Mechanism 3[9,17,25-28]:

$$Cu + Cl^- \Leftrightarrow CuCl + e^-$$

$$CuCl + Cl^- \Leftrightarrow CuCl_2^-$$

Table 1. Mathematical models of three reaction mechanisms

Mechanism	Mathematical Model	Author(s)
1	$i = F\left(\frac{D_{CuCl_2^-}}{\delta_N}\right)\left[Cl^-\right]^2 \exp\left(\frac{FE}{RT}\right)$	Bacarella Griess [13]
1	$i = \frac{zF\omega^{0.5}}{1.61\gamma^{0.667}} D_{CuCl_2^-}^{0.667}\left[Cl^-\right]^3 \exp\frac{F\left(E_e - E_e^0\right)}{RT}$	Faita et al. [14]
2	$i = zFc_{Cu^+}^{\chi=0}\left[k_2 \exp\left(\frac{\alpha_A F}{RT}\eta\right) - k_{-2}\exp\left(\frac{\alpha_C F}{RT}\eta\right)\right] + \frac{1.61 D_{Cu^+}^{-0.67}\gamma^{0.167}\omega^{0.5}}{c_{Cu^+}^{\chi=0}}$	de Sanchez Schiffrin [15]
2	$i = \frac{Fk_2 \exp\left(\frac{\alpha_1 FE}{RT}\right)}{1 + \left(\frac{k_{-2}\delta_N}{k_2\left[Cl^-\right]^2 D_{CuCl_2^-}}\right)\exp\left(\frac{-\alpha_{-1}FE}{RT}\right)}$	Smyrl [16]

3	$i=\frac{\left(\frac{k_4k_5}{k_{-4}}\right)\left[Cl^-\right]^2\exp\left(\frac{FE}{RT}\right)}{1+\left(\frac{\delta_N}{D_{CuCl_2^-}}\right)k_{-5}}$	Moreau[18]
3	$i=F\left\{k_4\left[Cl^-\right]\exp\left(\frac{\alpha_A FE}{RT}\right)\right\}+\frac{k_{-4}\exp\left(\frac{-FE}{RT}\right)}{k_4k_5}+\frac{k_{-4}k_{-5}\delta_N\exp\left(\frac{-FE}{RT}\right)}{k_4k_5\left[Cl^-\right]^2D_{CuCl_2^-}}$	Deslouis et al.[17]

In this research, the electrochemical corrosion characteristics of the coating in different environment was studied systematically by rotating ring-disk electrode, and a new reaction mechanism was proposed. Moreover, mathematical model for Tafel potential region was established based on the new reaction mechanism and derivation process was independent with the assumption of quasi-reversible charge transfer process.

2. EXPERIMENTAL SECTION

2.1 Experimental materials

The coating in the experiment was prepared by cold spray technology, and its principle is shown in Figure 1. In the cold spray process, a gas is accelerated to supersonic velocity in a de'Laval-type nozzle, i.e., a converging-diverging nozzle. The coating material is injected into the gas stream in powder form at the inlet of the nozzle, accelerated by the gas in the nozzle, and propelled toward the substrate to be coated. Above a certain particle velocity, which is characteristic for each respective powder material and its properties, the particles form a dense and solid adhesive coating on the substrate surface[29-32]. Technological parameter used in this experiment are as follows: spraying temperature 300°C, gas pressure 2.8MPa, spraying distance 20mm. The spray material is copper powder and Cu_2O powder, the matrix material is Q235 steel.

Most of the coating used in this research is 10%Cu_2O+90%Cu (mass ratio), except those investigating the effect of Cu_2O content.

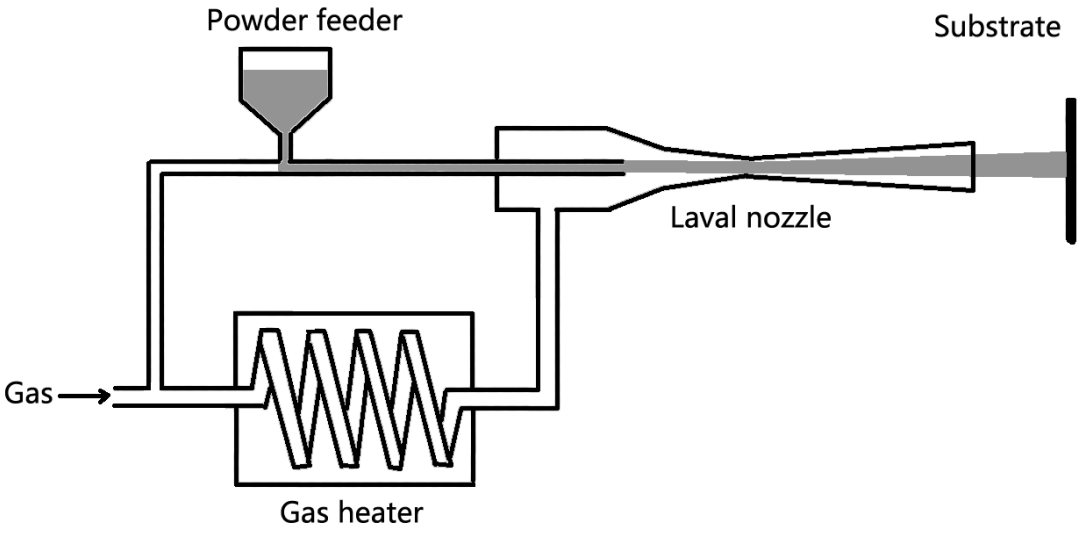

Figure 1. Schematic diagram of Cold Spray

2.2 Specimen processing

The specimens prepared by Cold Spray were cut into discs with 5mm-diameter, sanded lightly with 2000# sandpaper and then polished with W5.0 and W2.5 diamond polishing paste on metallographic polishing machine successively. Finally, wiped the surface of the coating with cotton balls moistened with ethanol, blow-dry, seal and store.

2.3 Rotating ring-disk electrode

The structure of rotating ring-disk electrode using in the experiment is shown in Figure 2 and the experimental specimen (Cold Spray Cu-Cu_2O Coating) is removable. Liquid was driven by the movement of the disc when it rotates around the axis perpendicular to its surface. The trajectory of the liquid could be obtained by the exact solution of Cochran's hydrodynamic equations[33]: liquid flow to the disc vertically at the place where away from the rotating disk, while liquid in the thin-layer close to the electrode surface rotate and its angular velocity increases as close to the disc until equal to the angular velocity of the disk.

Levich[33] obtained the convection diffusion equation of the rotating disk:

$$V_z(z)\frac{dc}{dz} = D\frac{d^2c}{dz^2}$$

Where, V_z is axial velocity component, D is diffusion coefficient, c is concentration.

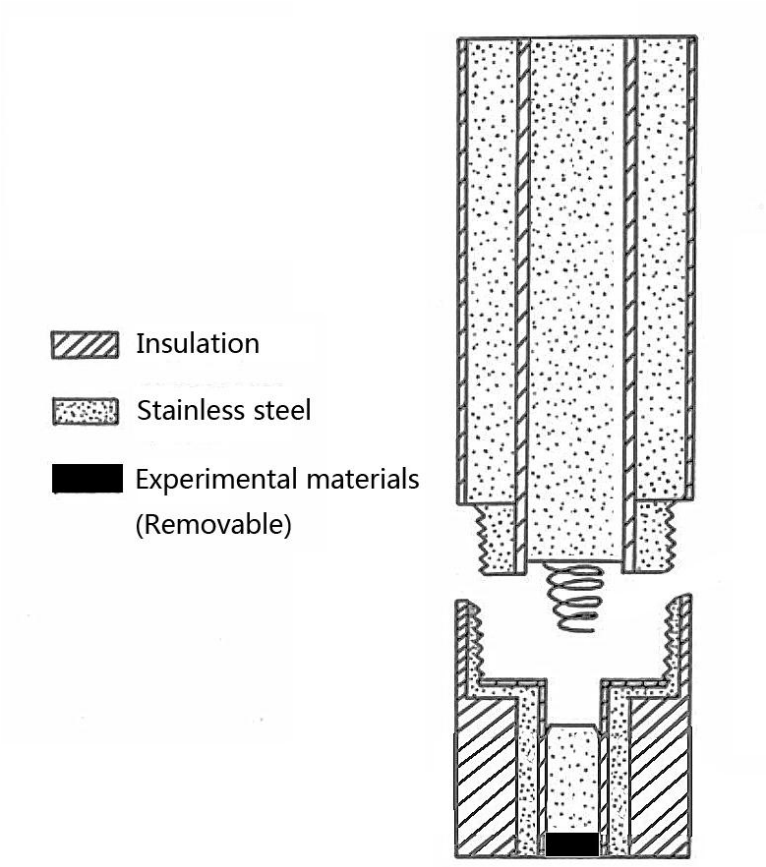

Figure 2. Structure diagram of rotating ring-disk electrode[34]

2.4 Electrochemical test system

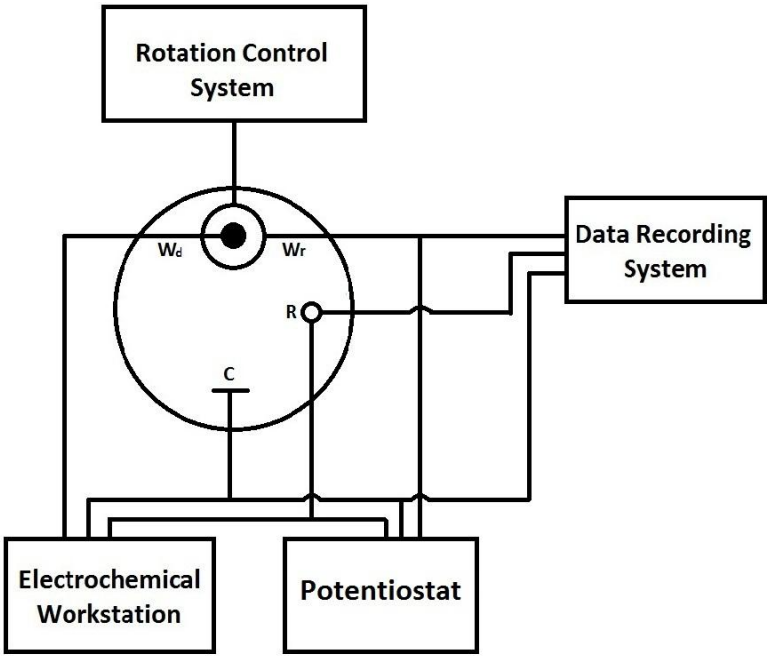

Figure 3. Schematic diagram of electrochemical test system

Fig.3 is the schematic diagram of electrochemical test system, where R is reference electrode, C is counter electrode, W_d is disc electrode, and W_r is ring electrode. Model 636 electrode rotation control instrument produced by Princeton Instruments CO., LTD. USA was used to control the electrode rotation speed. PAR 2273 electrochemical workstation (Princeton Instruments CO., LTD. USA) was used to polarize the disc electrode and record its electric potential and current. Ring electrode potential was set by DJS-292B potentiostat produced by Shanghai Xinrui Instruments & Meters CO., LTD. (detecting cuprous ion when set in 600mV and copper ions when -100mV). And PAR 273 electrochemical workstation produced by Princeton Instruments CO., LTD. USA served as data recording system to record current data of ring electrode.

2.5 Test influencing factors

The tests of electrode rotation speed ω, solution temperature T impact on the coating polarization proceeded in 3.5% NaCl solution. The tests of pH impact on the coating polarization proceeded in 0.5mol·L^{-1} NaCl solution. The temperature was controlled by thermostat water bath and pH was adjusted by NaOH and HCl solution.

In the tests of electrode rotation speed impact, ω was set at 191、318、637、1274、1910、2548、3184 revolutions·min^{-1} (rpm) respectively. They were 1200、2000、4000、8000、12000、16000、20000 rad·min^{-1} when converted into angular velocity.

A serial of NaCl solutions which concentration is 0.1、0.2、0.5、1.0、2.0、3.0、4.0mol·L^{-1} respectively were used to test the impact of Cl^- on the polarization of the coating. And all the experiment were carried out under the condition of 25°C, pH 8.0, and 8000 rad·min^{-1} electrode speed.

3. RESULTS AND DISCUSSION

Figure 4 shows the typical polarization curve of cold spray Cu-Cu_2O coating. The curve could be divided into four parts:

1. Anodic Tafel region ($Cu \rightarrow Cu^+$)
2. Limiting current region ($Cu \rightarrow Cu^+$)
3. Anodic high potential region (Cu^+, $Cu_2O \rightarrow Cu(II)$)
4. Cathodic polarization region (Cu^+, $Cu_2O \rightarrow Cu$ and reduction of oxygen)

In this paper, only the anode Tafel region will be discussed, and the other three will be reported in the following papers.

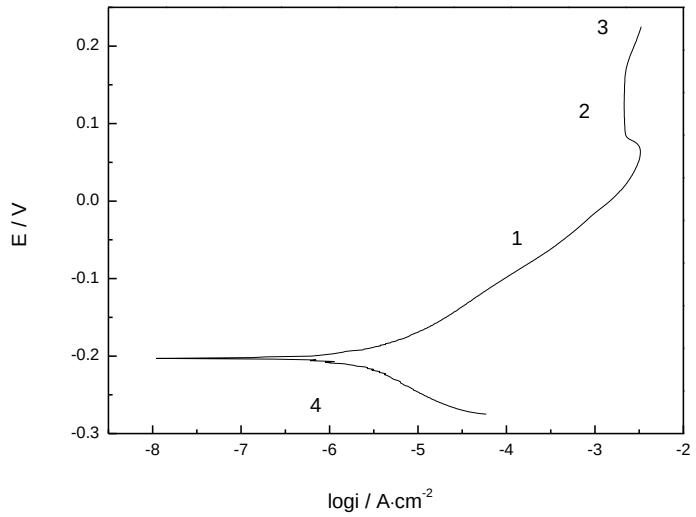

Figure 4. Typical anodic polarization curves of Cold Spray Cu-Cu_2O coating (10%Cu_2O, 3.5%NaCl, 25°C)

3.1 Influence of electrode rotating speed ω

Figure 5 shows the anodic Tafel polarization curves in different electrode speed. Potential (E) is linearly related to logarithmical current (logi) and the slope of the line increases with the increase of electrode rotation speed (figure 6), which means that control action of diffusion process is weakening and the effect of electrochemical control becomes more and more obvious in Tafel region when electrode rotation speed increases. In addition, the current in this whole region increases with the increase of electrode rotation speed. The variation of current along with electrode rotation speed at different potentials are shown in figure 7 which demonstrates that logi and logω are linearly related, and their slope are less than 0.5.

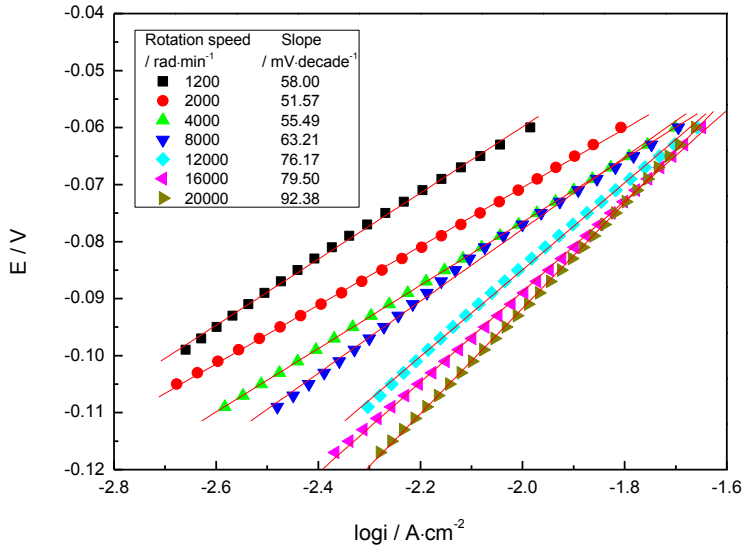

Figure 5. Anodic Tafel polarization curves in different electrode speed (3.5%NaCl, 25°C)

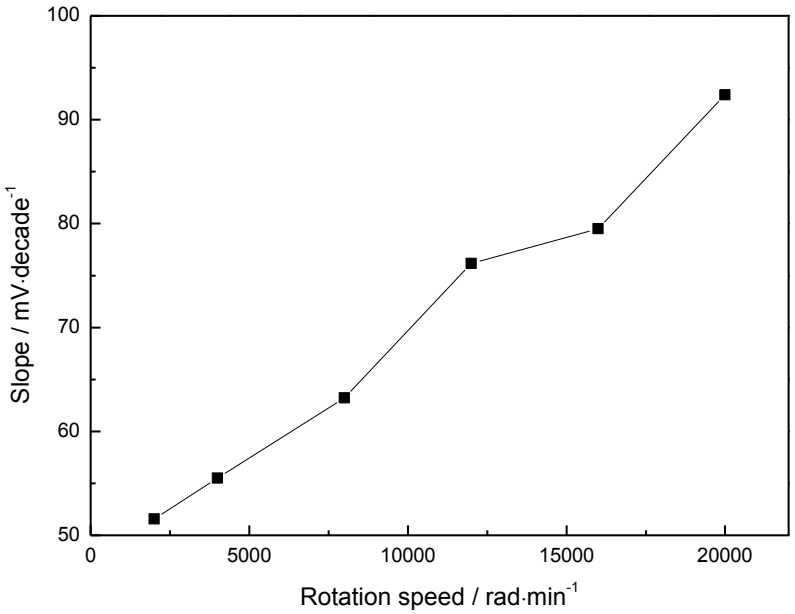

Figure 6. Variation of anodic Tafel slope with electrode rotation speed

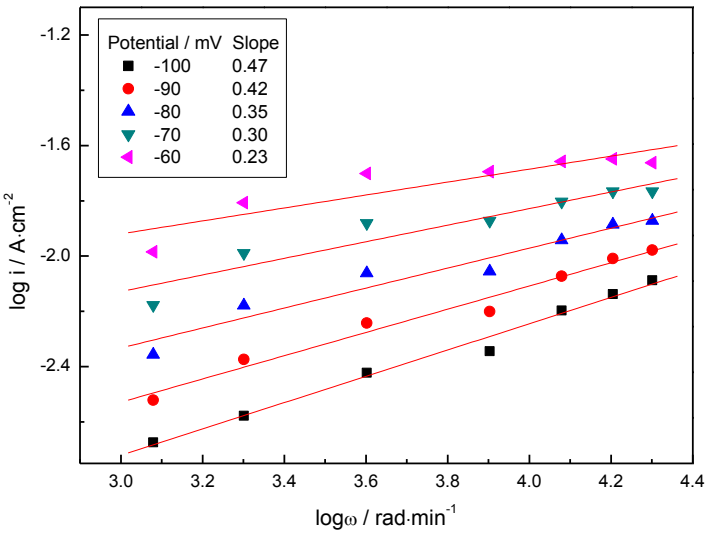

Figure 7. Relationship between logi and logω

3.2 Influence of Cl^- concentration

Relationship between Disc potential (E) and disc current (i) are shown in figure 8,while in figure 9, relationship between disc potential (E) and ring current (i_R) is illustrated. They are both linearly related with the slope of 60mV·decade^{-1}.

Both disc current and ring current increase with the increase of of [Cl^-]. From figure 10 and 11 we can tell that both logi-log[Cl^-] and logi_R-log[Cl^-] are linearly related, and their slope are 2.59 and 3.115 respectively.

Figure 12 shows logarithmic difference of i_R and i ($logi_R$-logi) of coatings with different percent component in NaCl solution with different concentration. The figure indicates that $logi_R$-logi values of pure copper coating maintain negative and exert independence of [Cl^-]. In coatings with Cu_2O, i_R is lower than i when Cl^- concentration is low. As [Cl^-] increasing, the $logi_R$-logi value becomes positive and i_R is greater than i. Moreover, in solution of the same concentration, the more Cu_2O the coating contains, the higher $logi_R$-logi value is.

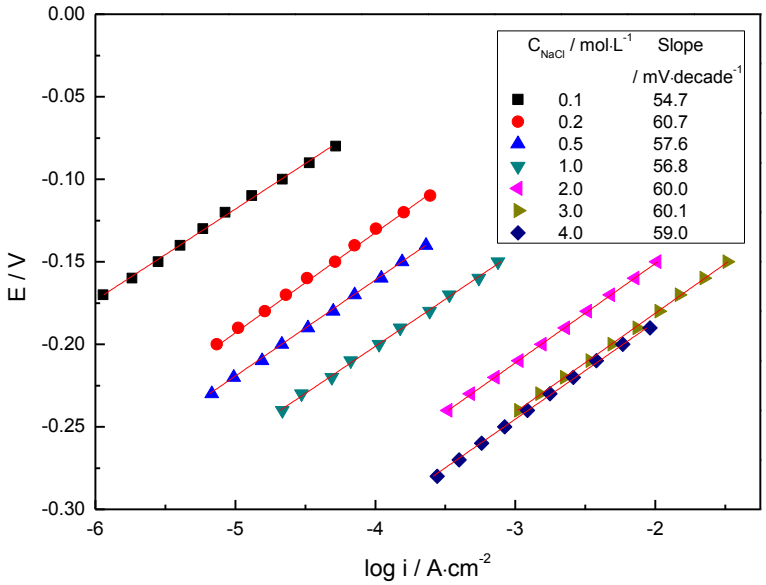

Figure 8. Anodic Tafel polarization curves in solution with different [Cl^-] (25°C, 8000 rad·min^{-1})

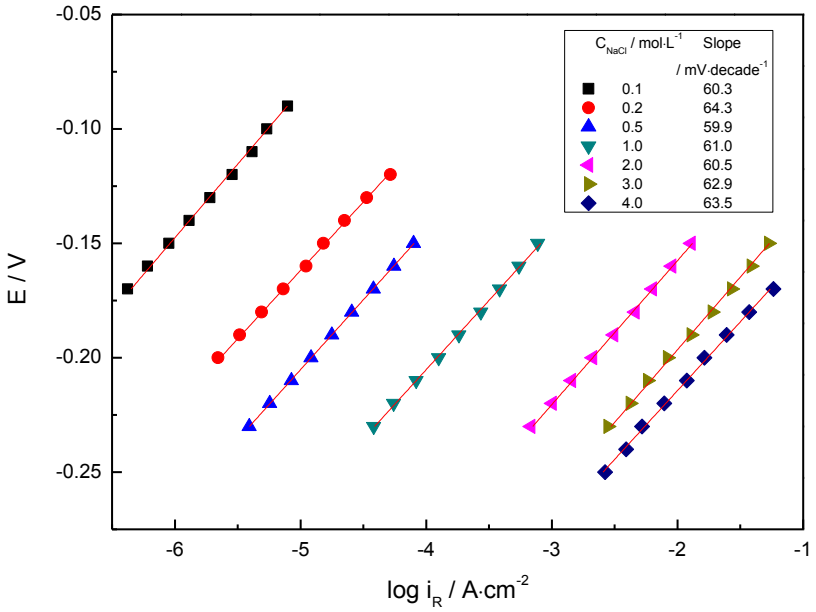

Figure 9. E - i_R curve in solution with different [Cl^-]in Tafel region (25°C, 8000 rad·min^{-1})

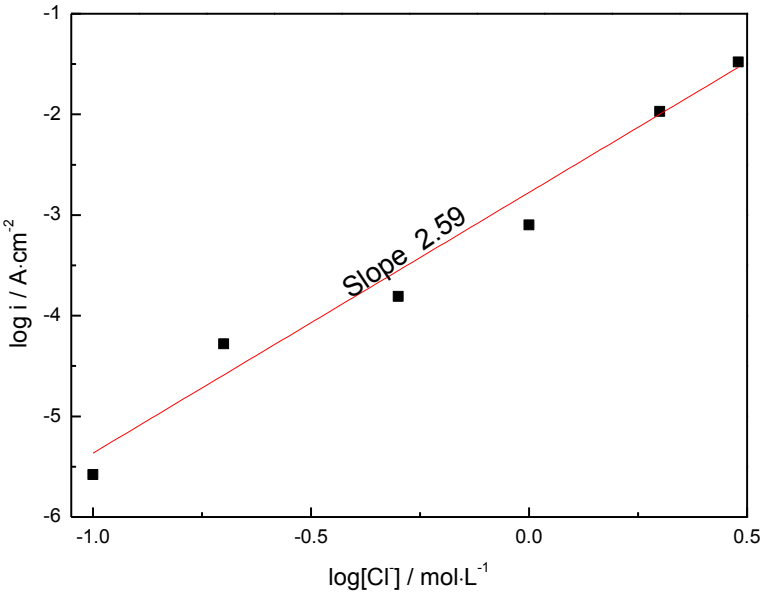

Figure 10. Relationship between log[Cl^-] and logi in Tafel region (-150mV)

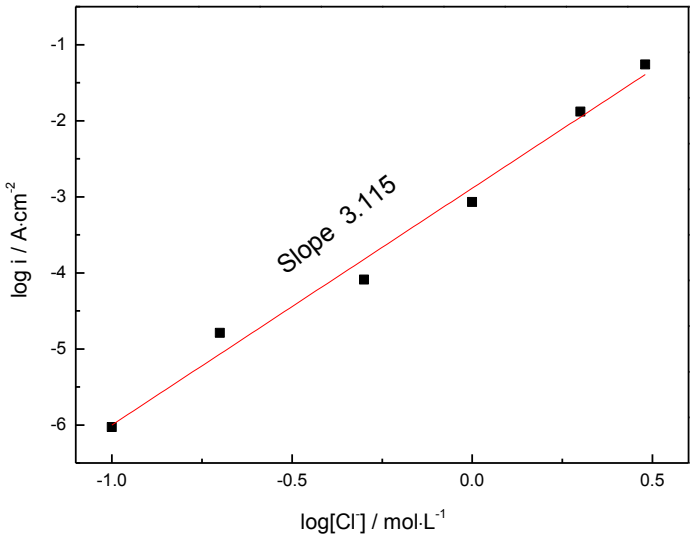

Figure 11. Relationship between log[Cl^-] and $logi_R$ in Tafel region (-150mV)

The above phenomenon can be explained by the following theory. i_R is generated when Cu is oxidized to Cu^+ on the disc electrode, while i derived when Cu^+ from the coatings is oxidized to Cu^{2+}. E is set at 600mV to detect Cu^+, thus, the Cu^+ detected by ring electrode include two parts,

$$Cu_2O + 4Cl^- + 2H^+ \rightarrow 2CuCl_2^- + H_2O$$

The reaction equation declare that increasing of Cl^- concentration promotes dissolution of Cu_2O and generates more Cu(I), so that the ring electrode detects more Cu(I) and produces greater ring current. This is the reason that slope of line $logi_R$-log[Cl^-] is bigger than line of logi-log[Cl-]. Also shows in figure 13, ring current i_R is less than disc current i when concentration of Cl^- is low because

of collection efficiency of ring electrode can not reach 100%. When concentration of Cl^- is high, the ring current i_R is greater than disc current i because of lots of Cu(I) generates by reaction of Cu_2O and large amount of Cl^-.

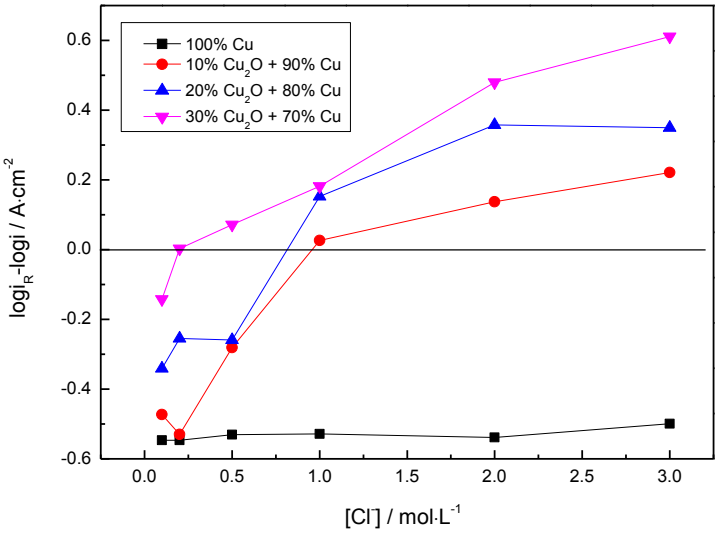

Figure 12. Variation of $logi_R$-logi value for coatings with different percent of Cu_2O content in solution with different NaCl concentration

3.3 Influence of temperature T

Figure 13 shows anodic Tafel polarization curves at different temperature. The potential of Tafel region shift negative along with elevation of temperature. At the same potential, the higher temperature is, the greater current is. This indicates the elevation of temperature promotes corrosion of coating, so that greater current generated at lower potential. Besides, the Tafel slope tends to increase following rising temperature.

Figure 14 shows measured values and theoretical values of Tafel slope under diffusion domination and electrochemical reaction domination. The measured values are coincident with theoretical values in tendency of changes following temperature. The measured values of Tafel slope is much lower than that under electrochemical reaction domination and a litter higher than theoretical values under diffusion domination. Measured values are more closer to theoretical values under diffusion domination, which indicates that electrode reaction is under control of both diffusion and electrochemical reaction, while diffusion control is more obvious. Moreover, as the increasing of temperature, measured values increasingly deviate from theoretical values of diffusion domination. Which may because the rise of temperature accelerates diffusion process, the role of diffusion domination is weakened and role of electrochemical reaction domination is enhanced.

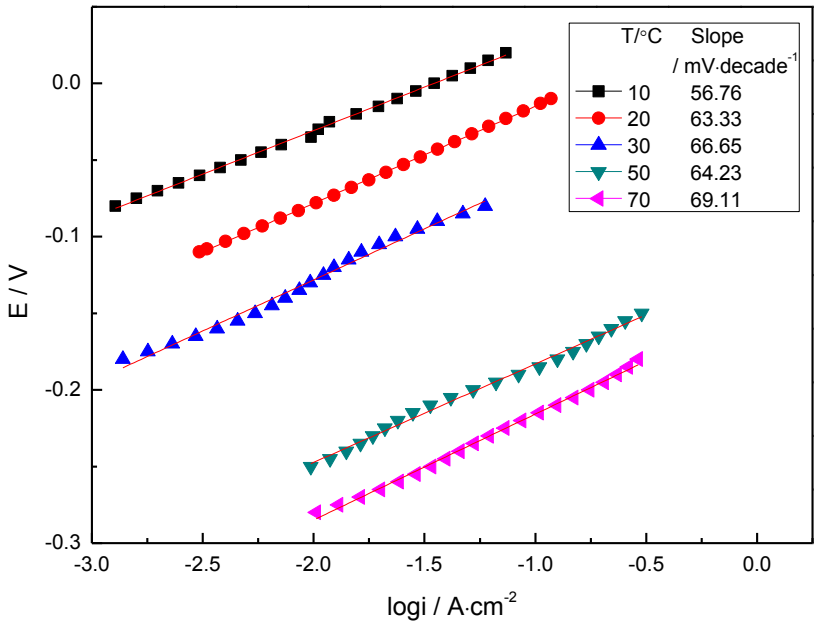

Figure 13. Anodic Tafel polarization curves at different temperature (3.5%NaCl, 8000 rad·min^{-1})

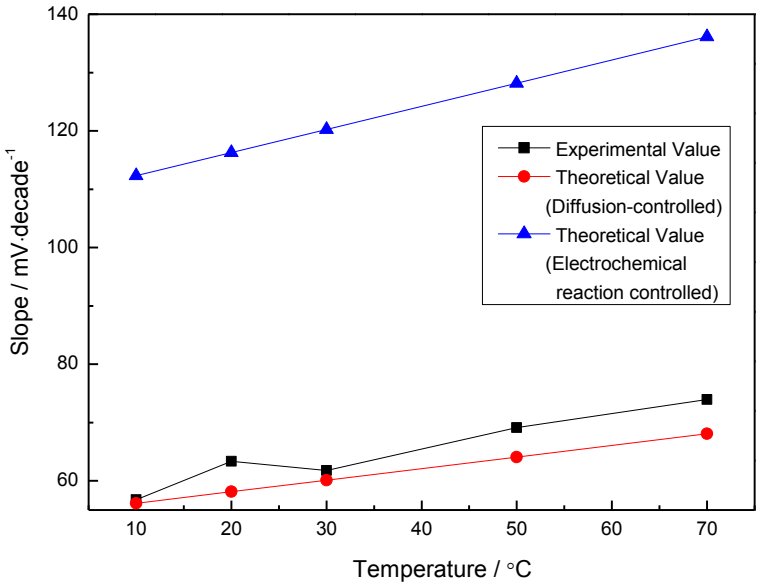

Figure 14. Experimental values and theoretical values of Tafel slope at different temperature

3.4 Influence of pH value

The anodic Tafel polarization curves at different pH values are shown in figure 15. The electrochemical dissolution of coating is independent from H^+ concentration and Tafel slopes remains at 60mV/decade. The current density are basically the same in acidic and neutral solutions at the same potential, while in alkaline environment, as shown in Figure 16, the current density are lower. That

may due to loose insoluble $Cu(OH)_2$ and $Cu_2(OH)_3Cl$ produced by OH^- and Cu(II) covers the surface of the coating and hinders the transfer of Cl^- and $CuCl_2^-$.

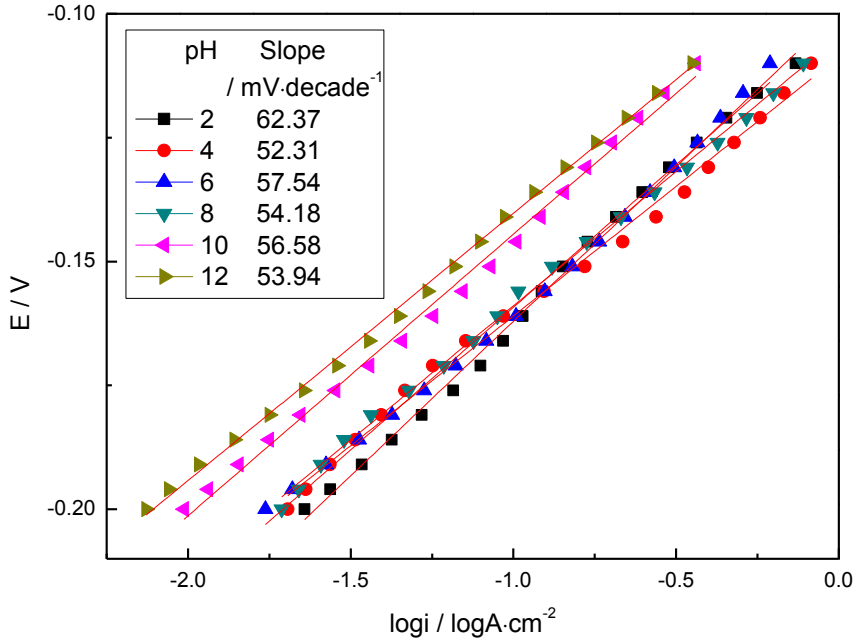

Figure 15. Anodic Tafel polarization curves in different pH condition (0.5mol·L^{-1} NaCl, 25°C, 8000 rad·min^{-1})

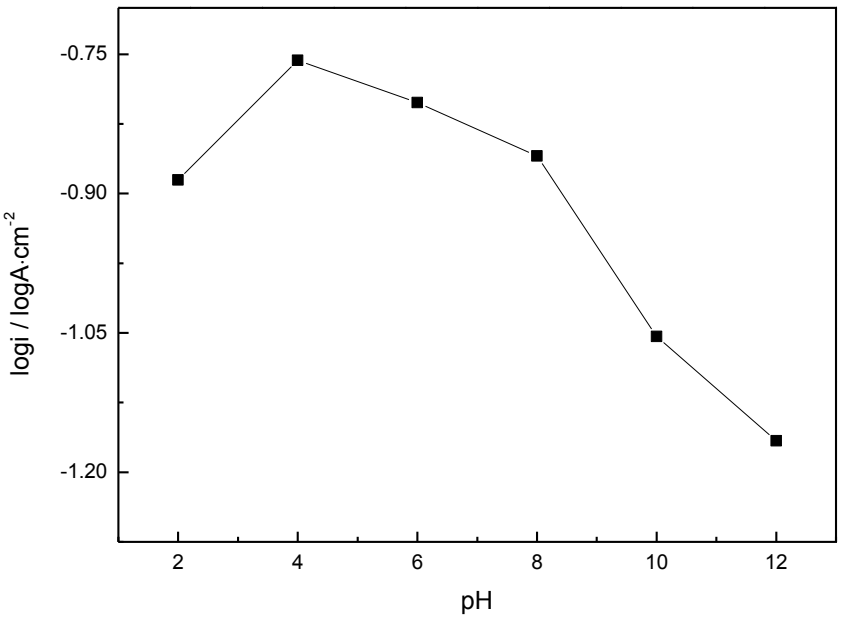

Figure 16. Logarithm of current density at different pH environment (Potential -150mV)

Figure 17 shows effect of pH on curves of disc potential-ring current in Tafel region. At the same potential, ring current increases with the decreasing of pH. Figure 18 shows logarithmic

difference between ring current and disc current (logi$_R$-logi) of coatings with different Cu_2O content at -150mV. The ring current is lower than disc current in alkaline condition while greater in acidic condition. At the same pH, the value of logi$_R$-logi increased with increase of Cu_2O in the coating. H^+ facilitates dissolution of Cu_2O and produces more $CuCl_2^-$. So ring current increases with decline of pH, and exceeds disc current finally. This is similar to the influence of Cl^- on value of logi$_R$-logi.

In pure copper coating with no Cu_2O content, the value of logi$_R$-logi does not change with pH. This indicates that H^+ does not effect the corrosion of coating in NaCl solution which is in accordance with results in figure 15 and conclusion of Claude Deslouis[35] and Moreau[18].

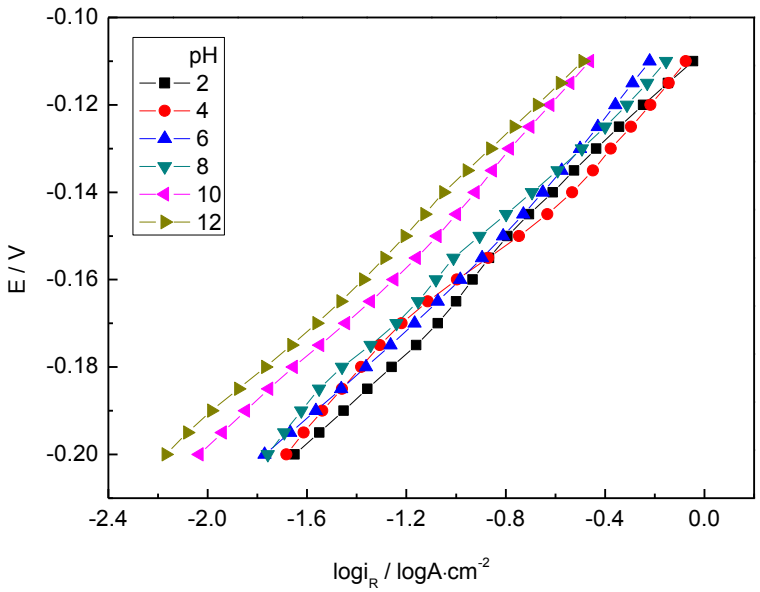

Figure 17. Effect of pH on curves of disc potential-ring current in Tafel region (0.5mol·L^{-1}, 25°C, 8000 rad·min^{-1})

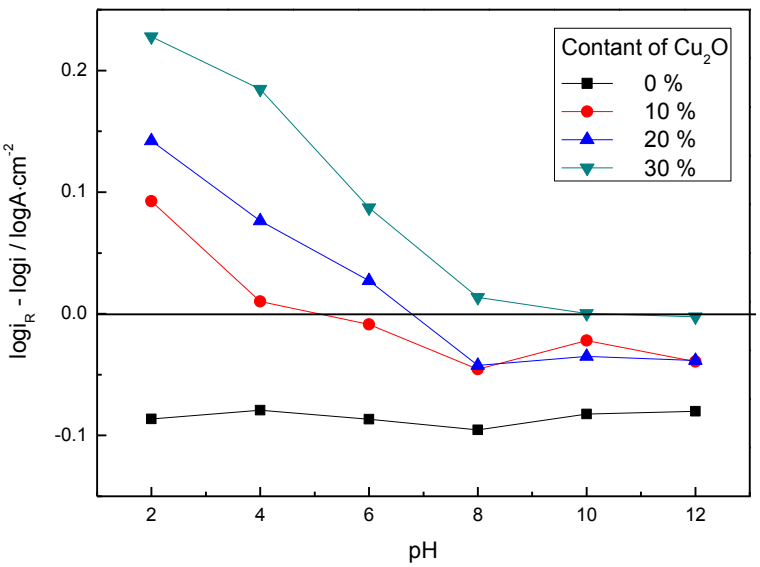

Figure 18. Function of pH and values of logi$_R$-logi for different coatings in which Cu_2O content vary from 0 to 30% (-150mV)

3.5 Reaction mechanism

When the coating is immersed in seawater, reactions on its surface are proceeding in three steps: (A) Cl^- is absorbed on the coating surface, (B) active anodic dissolution and formation of the oxide film, (C) dissolution of the oxide film.

Step (A) starts the whole reaction by absorbing Cl^- on the coating surface and formation of $(CuCl^-)_{ad}$, the reaction equation is as follows (A).

$$Cu + Cl^- \xrightarrow{k_1} CuCl^-_{ads} \quad \text{(A-1)}$$

Then the transition product $CuCl^-_{ads}$ reacts in two ways parallelly in step (B): (B1) adsorbs Cl^- and is oxidized into soluble anodic oxidation products, (B2) be oxidized into insoluble membrane directly without adsorption of Cl^-.

In (B1):

Transition product $CuCl^-_{ads}$ adsorbs Cl^- and is oxidized:

$$CuCl^-_{ads} + Cl^- \xrightarrow{k_2} CuCl^-_{2sur} + e^- \quad \text{(B1-1)}$$

$$CuCl^-_{2sur} \longrightarrow CuCl^-_{2sol} \quad \text{(B1-2)}$$

This is the anodic dissolution process of coating in seawater.

In (B2):

Transition product $CuCl^-_{ads}$ oxidizes to insoluble membrane directly without adsorption of Cl^-.

$$CuCl^-_{ads} \xrightarrow{k_3} CuCl_{ads} + e^- \quad \text{(B2-1)}$$

$$CuCl_{ads} \longrightarrow CuCl_{film} \quad \text{(B2-2)}$$

This is the formation process of the oxide film. Then the oxide film would be further Cu_2O film.

$$CuCl_{film} + H_2O \longrightarrow Cu_2O + 2H^+ + 2Cl^- \quad \text{(B2-3)}$$

In the final step (C), oxide film will be destroyed by chloride ion in the solution and dissolves.

$$CuCl_{film} + Cl^- \xrightarrow{k_4} CuCl^-_{2sur} \quad \text{(C-1)}$$

$$Cu_2O + 2H^+ + 4Cl^- \longrightarrow 2CuCl^-_2 + H_2O \quad \text{(C-2)}$$

And this is the dissolution of the oxide film.

3.6 Mathematical model of anodic Tafel region

The symbols used in this section are shown in Table 2.

Reaction (A-1) is an adsorption and desorption process which reacts rapidly and can reach the quasi equilibrium. Thus, it can be expressed by the equation below (1).

$$k_1[Cl^-] = k_{-1}[CuCl^-_{ads}] \quad (1)$$

Reaction (B1-1) is a charge transfer process. Generation rate of $CuCl_2^-$ can be described as follows (2),

$$r_{CuCl_2^-} = k_2[Cl^-][CuCl^-_{ads}]\exp(\frac{\alpha nFE}{RT}) - k_{-2}[CuCl^-_{2sur}]\exp[-\frac{(1-\alpha)nFE}{RT}] \quad (2)$$

Substitute Equation (1) into equation (2) and let the transfer coefficient α=0.5, and charge number n=1, equation (3) is obtained.

$$r_{CuCl_2^-} = \frac{k_1 k_2}{k_{-1}}[Cl^-]^2 \exp(\frac{FE}{2RT}) - k_{-2}[CuCl_{2sur}^-]\exp(-\frac{FE}{2RT}) \quad (3)$$

Reaction (B1-2) is the convection-diffusion process of ion $CuCl_2^-$ from electrode surface to solution which could be described by convection-diffusion equation[33] (4),

$$V_z(z)\frac{dc}{dz} = D\frac{d^2c}{dz^2} \quad (4)$$

where c is concentration of $CuCl_2^-$, and D is diffusion coefficient of ion $CuCl_2^-$ in this section.

Table 2. Symbol Description

k_1, k_2, k_3, k_4	Chemical reaction equilibrium constant
r	Formation rate or Consumption rate
α	Transfer coefficient
n	Charge number
F	Faraday constant
E	Electric potential
R	Universal gas constant
T	Thermodynamic temperature
V_z	Normal flow velocity
c	Concentration
z	Distance from electrode surface
ω	Angular velocity
γ	Dynamic viscosity
D	Diffusion coefficient
J	Diffusion rate
i	Current density

Furthermore z is the vertical distance from electrode surface, V_z is flow velocity in direction perpendicular to the electrode surface. Flow velocity V_z is a function of z[33], and the relationship between them can be expressed by equation (5).

$$V_z(z) \approx -0.51\omega^{3/2}\gamma^{-1/2}z^2 \text{ [33]} \quad (5)$$

where ω is electrode rotation speed, and γ is dynamic viscosity of solution.

Let $\frac{dc}{dz} = m$, equation (4) becomes

$$\frac{1}{m}dm = \frac{1}{D}V_z(z)dz \quad (6)$$

Integrate equation (6), and (7) can be obtained, where k is a coefficient.

$$\ln\frac{m}{k} = \frac{1}{D}\int_0^z V_Z(z)dz \quad (7)$$

When z=0,

$$k = m_{z=0} = (\frac{dc}{dz})_{z=0} \quad (8)$$

Then equation (7) can be written as follows,

$$\mathrm{m} = \frac{\mathrm{dc}}{\mathrm{dz}} = \mathrm{k}\exp[\frac{1}{\mathrm{D}}\int_0^{\mathrm{z}} \mathrm{V_Z(z)dz}] \quad (8)$$

Integrate equation (8), the result is shown by equation (9) (to distinguish the two intergrations, z in the first integral result is replaced by y.)[9]

$$c = k\int_0^z \exp[\frac{1}{D}\int_0^y V_y(y)dy]dz + B \quad (9)$$

where B is a constant.

Boundary condition 1: when z=∞, c=0 [9]. Thus,

$$0 = k\int_0^\infty \exp[\frac{1}{D}\int_0^y V_y(y)dy]dz + B \quad (10)$$

$$B = -k\int_0^\infty \exp[\frac{1}{D}\int_0^y V_y(y)dy]dz \quad (11)$$

Concentration expression of $CuCl_2^-$ is obtained by substituting Equation (11) into equation (9),

$$\mathrm{c} = \mathrm{k}\int_0^{\mathrm{z}} \exp[\frac{1}{\mathrm{D}}\int_0^{\mathrm{y}} \mathrm{V_y(y)dy}]\mathrm{dz} - \mathrm{k}\int_0^\infty \exp[\frac{1}{\mathrm{D}}\int_0^{\mathrm{y}} \mathrm{V_y(y)dy}]\mathrm{dz} \quad (12)$$

when z=0,

$$\mathrm{c_{z=0}} = -\mathrm{k}\int_0^\infty \exp[\frac{1}{\mathrm{D}}\int_0^{\mathrm{y}} \mathrm{V_y(y)dy}]\mathrm{dz} \quad (13)$$

Boundary condition 2 [9]: At steady-state balance and the point z=0, generating rate of $[CuCl_2^-]$ equals to its diffusion rate but in the opposite direction, no matter the dominant reaction is diffusion process or electrochemical reaction.

$$J_{z=0} = D(\frac{dc}{dz})_{z=0} = -\mathrm{r_{CuCl_2^-(z=0)}} \quad (14)$$

Equation 15 is derived by substituting (3), (8) and (13) into (14),

$$k = -\frac{\frac{k_1 k_2}{k_{-1}}[Cl^-]^2 \exp(\frac{FE}{RT})}{k_{-2}\int_0^\infty \exp[\frac{1}{D}\int_0^y V_y(y)dy]dz \exp(-\frac{FE}{2RT}) + D} \quad (15)$$

Expression above contains an integration which is

$$\int_0^\infty \exp[\frac{1}{\mathrm{D}}\int_0^{\mathrm{y}} \mathrm{V_y(y)dy}]\mathrm{dz} \quad (16)$$

Firstly, calculate a part of equation (16), which is

$$\int_0^{\mathrm{y}} \mathrm{V_y(y)dy} \quad (17)$$

Then, substituting equation (5) into equation (17) and get (18),

$$\int_0^y V_y(y)dy = -0.51\omega^{3/2}\gamma^{-1/2}\int_0^y y^2 dy = -\frac{0.51\omega^{3/2}\gamma^{-1/2}y^3}{3} \quad (18)$$

Next, substituting equation (18) into equation (16) and get (19),

$$\int_0^\infty e^{-bz^3}dz = \int_0^\infty e^{-(b^{1/3}z)^3}dz = \frac{1}{b^{1/3}}\int_0^\infty e^{-(b^{1/3}z)^3}d(b^{1/3}z) \quad (19)$$

where $b = \frac{0.51\omega^{3/2}\gamma^{-1/2}}{3D}$. Let $x=b^{1/3}z$, and equation (19) can be written as follows

$$\frac{1}{b^{1/3}}\int_0^\infty e^{-x^3}dx = \frac{1}{3b^{1/3}}\int_0^\infty e^{-x^3}(x^3)^{-2/3}dx^3 \quad (20)$$

Let $t=x^3$, and equation (20) becomes

$$\frac{1}{3b^{1/3}}\int_0^\infty e^{-t}t^{-2/3}dt = \frac{1}{b^{1/3}}\Gamma(\frac{4}{3}) = 1.6D^{\frac{1}{3}}\omega^{-\frac{1}{2}}\gamma^{\frac{1}{6}} \quad (21)$$

where $\Gamma(x)$ is Gamma function and $\Gamma(4/3)=0.8934$. Thus, the solution of integration (16) is equation (21). Then equation (22) is obtained via substituting equation (21) into equation (15),

$$k = -\frac{\frac{k_1k_2}{k_{-1}}[Cl^-]^2\exp(\frac{FE}{2RT})}{D+1.6k_{-2}D^{\frac{1}{3}}\omega^{-\frac{1}{2}}\gamma^{\frac{1}{6}}\exp(-\frac{FE}{2RT})} = -\frac{\frac{k_1k_2}{k_{-1}}[Cl^-]^2\exp(\frac{FE}{RT})}{D\exp(\frac{FE}{2RT})+1.6k_{-2}D^{\frac{1}{3}}\omega^{-\frac{1}{2}}\gamma^{\frac{1}{6}}} \quad (22)$$

Current i can be expressed by generation rate r of $CuCl_2^-$,

$$i = nFr_{CuCl_2^-(z=0)} = -nFJ_{z=0} = -FD(\frac{dc}{dz})_{z=0} = -FDk$$

$$= FD\frac{\frac{k_1k_2}{k_{-1}}[Cl^-]^2\exp(\frac{FE}{RT})}{D\exp(\frac{FE}{2RT})+1.6k_{-2}D^{\frac{1}{3}}\omega^{-\frac{1}{2}}\gamma^{\frac{1}{6}}} \quad (23)$$

Equation (23) is the expression of anodic Tafel polarization current which includes both control factors of diffusion and electrochemical reaction.

Compare equation (23) and H.P.Lee's result (the following equation), the latter defaulted the electrode process was controlled by diffusion, without considering the electrochemical reaction control factors.

$$i = FD\frac{\frac{k_1k_2}{k_{-1}}\left[Cl^-\right]\exp\left(\frac{FE}{RT}\right)}{D+1.6k_{-2}D^{\frac{1}{3}}\omega^{-\frac{1}{2}}\gamma^{\frac{1}{6}}}$$

Equations below can be derived from equation (23)

$$59mV\cdot decade^{-1} = \frac{2.303RT}{F} \le \frac{dE}{d\log i} \le \frac{2\times 2.303RT}{F} = 118mV\cdot decade^{-1} \quad (24)$$

$$\frac{d\log i}{d\log[Cl^-]} = 2 \quad (25)$$

$$\frac{d\log i}{d\log\omega} < 0.5 \quad (26)$$

When $\omega\to\infty$,diffusion process is so rapid that current is controlled by electrochemical reaction. Therefore the term $1.6k_{-2}D^{1/3}\omega^{-1/2}\gamma^{1/6}$ in equation (23) can be omitted. Then equation (23) becomes

$$i = F\frac{k_1 k_2}{k_{-1}}[Cl^-]^2 \exp(\frac{FE}{2RT}) \quad (27)$$

According to equation (27),

$$\frac{dE}{d\log i} = \frac{2\times 2.303RT}{F} = 118mV\cdot decade^{-1} \quad (28)$$

When $\omega\to 0$, the role of diffusion-control is not obvious and the value of item $1.6k_{-2}D^{1/3}\omega^{-1/2}\gamma^{1/6}$ is so large that term Dexp(FE/2RT) can be omitted. Equation (23) becomes

$$i = 0.625\frac{k_1 k_2}{k_{-1}k_{-2}}FD^{\frac{2}{3}}\omega^{\frac{1}{2}}\gamma^{-\frac{1}{6}}[Cl^-]^2 \exp(\frac{FE}{RT}) \quad (29)$$

Then,

$$\frac{dE}{d\log i} = \frac{2.303RT}{F} = 59mV\cdot decade^{-1} \quad (30)$$

$$\frac{d\log i}{d\log \omega} = 0.5 \quad (31)$$

Figure 5 and 6 shows that the functional relationship between Tafel slope and electrode rotation speed ω is in accordance with the theoretical results of equation (24), (28) and (30). It indicates that the role of diffusion control is weakened while electrochemical reaction control becomes more and more obvious along with the increase of electrode rotation speed.

The experimental results revealed in figure 7 agrees with the theoretical result of equation (26), which suggests that corrosion of coating is dominated by diffusion process and electrochemical reaction both in Tafel region.

The experimental results shown in figue 10

$$\frac{d\log i}{d\log[Cl^-]} = 2.59$$

$$\frac{d\log i_R}{d\log[Cl^-]} = 3.115$$

deviates from the theoretical result of equation (25) slightly, which is due to the dissolve of Cu_2O component in the coating under the action of the Cl^-.

3.7 Diffusion - limiting species

In the previous discussion, $CuCl_2^-$ is assumed to be the diffusion - limiting species in Tafel region. There is another case that the limiting diffusion species maybe Cl^-. Then mathematical model based on hypothesis that Cl^- is the diffusion - limiting species would be discussed in this section. The diffusion of Cl^- from solution to electrode surface happened first all of.

$$Cl^-_{sol} \longrightarrow Cl^-_{sur} \quad (32)$$

Diffusion process (32) could be described by convection-diffusion equation (33) where D, c are diffusion coefficient and concentration of Cl^- respectively in this section.

$$V_z(z)\frac{dc}{dz} = D\frac{d^2c}{dz^2} \quad (33)$$

The adsorption and desorption reaction (A-1) is rapid and reach the quasi equilibrium. So,

$$k_1[Cl^-] = k_{-1}[CuCl^-_{ads}] \quad (34)$$

Consumption rate of Cl^- in reaction (B1-1) could be described by the equation bellow.

$$r_{Cl^-} = k_2[Cl^-][CuCl^-]\exp(\frac{\alpha nFE}{RT}) - k_{-2}[CuCl_2^-]\exp[-\frac{(1-\alpha)nFE}{RT}] \quad (35)$$

Let coefficient α=0.5 and charge number n=1, it becomes

$$r_{Cl^-} = k_2[Cl^-][CuCl^-]\exp(\frac{FE}{2RT}) - k_{-2}[CuCl_2^-]\exp[-\frac{FE}{2RT}] \quad (36)$$

Because [Cl-]>>[$CuCl_2^-$], and $CuCl_2^-$ is assumed to be non-limiting diffusion species, the equation above could be simplified as

$$r_{Cl^-} = k_2[Cl^-][CuCl^-]\exp(\frac{FE}{2RT}) \quad (37)$$

Equation (38) is derived by substituting equation (34) into equation (37),

$$r_{Cl^-} = \frac{k_1k_2}{k_{-1}}[Cl^-]^2\exp(\frac{FE}{2RT}) \quad (38)$$

Expression of Cl^- concentration is obtained by quadratic integral of convection-diffusion equation (33), where k is a coefficient and B is a constant.

$$c = k\int_0^z \exp[\frac{1}{D}\int_0^y V_y(y)dy]dz + B \quad (39)$$

$$k = \left(\frac{dc}{dz}\right)_{z=0} \quad (40)$$

Boundary condition 1: when $z=\infty$, $c=c_0$ (c_0 is concentration of Cl^- in solution)[9]. Then,

$$B = c_0 - k\int_0^\infty \exp[\frac{1}{D}\int_0^y V_y(y)dy]dz \quad (41)$$

Substitute (41) into (39),

$$c = c_0 + k\left\{\int_0^z \exp[\frac{1}{D}\int_0^y V_y(y)dy]dz - \int_0^\infty \exp[\frac{1}{D}\int_0^y V_y(y)dy]dz\right\} \quad (42)$$

Concentration of Cl^- on the electrode surface (z=0) is

$$c_{z=0} = c_0 - k\int_0^\infty \exp[\frac{1}{D}\int_0^y V_y(y)dy]dz \quad (43)$$

Boundary condition 2 [9]: When z=0 (that is electrode surface), diffusion rate of Cl^- J_{Cl^-} is equal to the rate of consumption r_{Cl^-} and in the opposite direction when reaches steady-state balance.

$$J_{Cl^-(z=0)} = -D\left(\frac{dc}{dz}\right)_{z=0} = -Dk = -r_{Cl^-(z=0)} = -\frac{k_1k_2}{k_{-1}}[Cl^-]^2_{z=0}\exp(\frac{FE}{2RT}) \quad (44)$$

Substitute (43) and (44),

$$Dk = \frac{k_1k_2}{k_{-1}}\exp(\frac{FE}{2RT})\left\{c_0 - k\int_0^\infty \exp[\frac{1}{D}\int_0^y V_y(y)dy]dz\right\}^2 \quad (45)$$

From equation (16)~(21) it can be knew that,

$$\int_0^{\infty} \exp[\frac{1}{D}\int_0^{y} V_y(y)dy]dz = 1.62D^{\frac{1}{3}}\gamma^{\frac{1}{6}}\omega^{-\frac{1}{2}} = M \quad (46)$$

Substitute (46) into (45) and let $K_0 = \frac{k_1 k_2}{k_{-1}}$.

$$M^2 \exp(\frac{FE}{2RT})k^2 - [\frac{D}{K_0} + 2c_0 M \exp(\frac{FE}{2RT})]k + c_0^2 \exp(\frac{FE}{2RT}) = 0 \quad (47)$$

Multiply (47) by k^{-2} and let q=1/k, equation (47) becomes

$$c_0^2 \exp(\frac{FE}{2RT})q^2 - [\frac{D}{K_0} + 2c_0 M \exp(\frac{FE}{2RT})]q + M^2 \exp(\frac{FE}{2RT}) = 0 \quad (48)$$

Expression of q is obtained by solving equation (48)

$$q = \frac{\frac{D}{K_0} + 2c_0 M \exp(\frac{FE}{2RT}) \pm \left\{\left[\frac{D}{K_0} + 2c_0 M \exp(\frac{FE}{2RT})\right]^2 - 4c_0^2 M^2 \exp(\frac{FE}{RT})\right\}^{\frac{1}{2}}}{2c_0^{\ 2} \exp(\frac{FE}{2RT})}$$

$$= \frac{\frac{D + 2c_0 M K_0 \exp(\frac{FE}{2RT})}{K_0} \pm \left[\frac{D}{K_0} \times \frac{D + 4c_0 M K_0 \exp(\frac{FE}{2RT})}{K_0}\right]^{\frac{1}{2}}}{2c_0^{\ 2} \exp(\frac{FE}{2RT})} \quad (49)$$

Then the numerator and denominator of equation (49) are multiplied by K_0D^{-1} simultaneously, it is simplified as

$$q = \frac{\left[2c_0 M K_0 D^{-1} \exp(\frac{FE}{2RT}) + 1\right] \pm \left[4c_0 M K_0 D^{-1} \exp(\frac{FE}{2RT}) + 1\right]^{\frac{1}{2}}}{2c_0^2 K_0 D^{-1}} \quad (50)$$

Square root in the form of $(1+x)^{\frac{1}{2}}$ can be expressed as power series bellow [9].

$$(1+x)^{\frac{1}{2}} = 1 + \frac{x}{2} - \frac{x^2}{8} + \frac{x^3}{16} - \ldots\ldots \quad (51)$$

When x<<1, the above equation can be simplified as

$$(1+x)^{\frac{1}{2}} = 1 + \frac{x}{2} \quad (52)$$

Because of $4c_0MK_0D^{-1}\exp(FE/2RT)<<1$, equation (50) becomes

$$q = \frac{\left[2c_0 M K_0 D^{-1} \exp(\frac{FE}{2RT}) + 1\right] \pm \left[2c_0 M K_0 D^{-1} \exp(\frac{FE}{2RT}) + 1\right]}{2c_0^2 K_0 D^{-1}} = \frac{2c_0 M K_0 D^{-1} \exp(\frac{FE}{2RT}) + 1}{c_0^2 K_0 D^{-1}} \quad (53)$$

Current i can be expressed as function of diffusion rate r of Cl^-,

$$i = -n_1 F J_{Cl^-} = F J_{Cl^-} = -FDk = -\frac{FD}{q} \quad (54)$$

Substitute equation (46) and (53) into (54),

$$i = -\frac{Fc_0^2 K_0}{3.24 c_0 K_0 D^{-2/3}\omega^{-1/2}\gamma^{1/6}\exp\left(\frac{FE}{2RT}\right)+1} = -\frac{F[Cl^-]^2\frac{k_1k_2}{k_{-1}}}{3.24\frac{k_1k_2}{k_{-1}}[Cl^-]D^{-2/3}\omega^{-1/2}\gamma^{1/6}\exp\left(\frac{FE}{2RT}\right)+1} \quad (55)$$

Then (56) can be obtained from equation (55),

$$\frac{dE}{d\log i} \le -\frac{2\times 2.303RT}{F} = -118mV\cdot decade^{-1} \quad (56)$$

$$1 < \frac{d\log i}{d\log[Cl^-]} < 2 \quad (57)$$

The above equations do not match the experimental results shown in figure 5, 10 and 11. Thus, the limiting diffusion species is not Cl^- but $CuCl_2^-$.

4. CONCLUSIONS

The formation of $(CuCl^-)_{ad}$ by adsorpting Cl^- on the coating surface start the whole reaction. Then $(CuCl^-)_{ad}$ reacts in two competitive progresses which are active anodic dissolution and formation of the oxide film.

The mathematical model based on the reaction mechanism established in this research accords well to the experimental results, which demonstrates the rationality of mathematical model and reaction mechanism.

The corrosion of Cold Spray Cu-Cu_2O coating is under the control of diffusion process and electrochemical reaction both in Tafel region. And the limiting diffusion species is $CuCl_2^-$.

The increase of $[Cl^-]$ accelerates the dissolution of Cu_2O. Thisfacilitates the release of toxins and improvement of antifouling effect, but exacerbates the corrosion too.

The change of pH does not influence the corrosion mechanism of the coating. But the decrease of pH makes Cu_2O dissolved more quickly, which is conducive to the release of toxins and improvement of antifouling effect.

References

1. Ding Rui, Li Xiangbo, Wang Jia, Xu Likun, *Corrosion Science & Protection Technology*, 24 (2012) 173.
2. Jutta Elguindi, Stuart Moffitt, Henrik Hasman, Cassandra Andrade, Srini Raghavan, Christopher Rensing, *Applied Microbial and Cell Physiology*, 89 (2011) 1963.
3. K.F. Khaled, *Materials Chemistry and Physics*, 125 (2011) 427.
4. Chen J, Qin Z, Shoesmith D W, *Corrosion Engineering, Science and Technology*, 46 (2011) 138.
5. Ji Eun Lee, Hyun Dong Lee, Gi Eun Kim, *Environmental Engineering Research*, 17(2012) 17.
6. M. M. Antonijevic, M. B. Petrovic, *Int. J. Electrochem. Sci*, 3 (2008) 1.
7. Yeganeh. M, Saremi. M, *Micro & Nano Letters*, 6(2011) 26.
8. Digby D, Macdonald, Samin Sharifi, Jan Linder, *Meet. Abstr*, 2 (2011) 1748.
9. H.P. Lee, K. Nobe, *Journal of the Electrochemical Society*, 133 (1986) 2035.
10. Xiaoning Liao, Fahe Cao, Liyun Zheng, Wenjuan Liu, Anna Chen, Jianqing Zhang, Chunan Cao, *Corrosion Science*, 53 (2011) 3289.

11. M. Braun, K. Nobe, *Journal of the Electrochemical Society*, 126 (1979) 1666.
12. G. Bianchi, G. Fiori, P. Longhi, F. Mazza, *Corrosion-NACE*, 34 (1978) 396.
13. G. Faita, G. Fiori, D. Salvadore, *Corrosion Science*, 15 (1975) 383.
14. A.L. Bacarella, J.C. Griess Jr., *Journal of the Electrochemical Society*, 120 (1973) 459.
15. S.R. de Sanchez, D.J. Schiffrin, *Corrosion Science*, 22 (1982) 585.
16. W.H. Smyrl, *Journal of the Electrochemical Society*, 132 (1985) 1556.
17. C. Deslouis, B. Tribollet, G. Mengoli, M. Musiani, *Journal of Applied Electrochemistry*, 18 (1988) 374.
18. A. Moreau, *Electrochimica Acta*, 26 (1981) 497.
19. S.R. de Sanchez, D.J. Schiffrin, *Corrosion Science*, 28 (1988) 141.
20. R.J.K. Wood, S.A. Fry, *Journal of Fluids Engineering—Transactions*, 112 (1990) 218.
21. J. Mathiyarasu, N. Palaniswamy, V.S. Muralidharan, *Proceedings of the Indian Academy of Sciences-Chemical Sciences*, 111 (1999) 377.
22. Da-Quan Zhang, Qi-Rui Cai, Xian-Ming He, Li-Xin Gao, Guo-Ding Zhou, *Materials Chemistry and Physics*, 112 (2008) 353.
23. B. Tribollet, J. Newman, *Journal of the Electrochemical Society*, 131 (1984) 2780.
24. G. Kear, F.C. Walsh, D.B. Barker, K.S. Stokes, *Leighton Buzzard*, UK (2000).
25. M.E. Walton, P.A. Brook, *Corrosion Science*, 17 (1977) 317.
26. M. Georgiadou, R. Alkire, *Journal of Applied Electrochemistry*, 28 (1998) 127.
27. F. King, M.J. Quin, C.D. Litke, *Journal of Electroanalytical Chemistry*, 385 (1995) 45.
28. R.K. Flatt, P.A. Brook, *Corrosion Science*, 11 (1971) 185.
29. Alkimov A P, Kosarev V F, Papyrin A N, *Dokl Akad Nauk SSSR*, 315(1990) 1062.
30. Blose R E, Roemer T J, Orlando: ASM (2003).
31. Karthikeyan J, Kay CM, Orlando: ASM (2003).
32. T. Stoltenhoff, H. Kreye, and H.J. Richter, *Journal of Thermal Spray Technology*, 11 (2002) 542.
33. Levich, Prentice Hall, Inc., Englewood. NJ (1962).
34. H. P. Lee, Ken Nobe, *J. Elctrochem. Soc.*, 131 (1984) 1236.
35. Claude Deslouis, Bernard Tribollet, Guiliano Mengoli, Marco M. Musiani, *Journal of Applied Electrochemistry* 18 (1988) 374.